Blast wave formation during ballistic impact of consolidated metal powder projectiles

Jordan Tubman, Dihia Idrici, Victor Muckensturm, Samuel Goroshin, and David L. Frost
McGill University, Mechanical Engineering Department, Montreal, Quebec, Canada

Jason Loiseau,
Royal Military College, Department of Chemistry and Chemical Engineering, Kingston, Ontario, Canada

1 Introduction

The impact of a supersonic projectile with a rigid target is a complex multistage process involving the projectile deformation and fragmentation, light emission, and the formation of a blast wave that propagates away from the target. The nature and duration of the light emission, as well as the type of energy that influences the peak strength of the blast wave depends on several variables, including projectile velocity and material properties. For reactive metal projectiles the impact may initiate chemical reactions between the fragments and the surrounding oxygen, depositing additional chemical energy into the system. Within the explosively-launched regime (i.e., ~0.5 – 2 km/s), the specific chemical energy associated with complete oxidation of the metal is more than an order of magnitude greater than the specific kinetic energy, as shown by Idrici et al. [1].

Extensive previous work has been carried out to characterize the impact flash and fragmentation of projectiles during ballistic impact. For example, Simpson et al. [2] studied the impact flash during the impact of spherical steel projectiles in vacuum. They found a mechanistic connection between the impact flash and the ejecta cone, with the fragmented particles in the ejecta cone driving the impact flash. While much of previous work utilized bulk metal projectiles, some researchers have investigated the impact of consolidated powder projectiles, with a focus on the effect of material properties on the distribution of the fragment sizes generated. For example, Hooper [3] accelerated compacted aluminum powder spheres through thin steel perforation plates and captured the fragments for analysis. He found that as the velocity increased, the fragment distribution transitioned from the typical exponential form into a power-law form. A subsequent study considered the impact of compacted zinc cylinders on an aluminum target [4]. The fragments from this study did not display the power-law behaviour seen with compacted aluminum, and instead followed a distribution proposed by Mott and Linfoot [5]. While the compacted projectiles in [3, 4] were both annealed, a study by Kline and Hooper [6] specifically looked at the effect of mild annealing on the fragmentation of compacted aluminum projectiles. Exposing the projectiles to even short periods of low temperatures (200°C) significantly increased the compacted projectiles' ductility.

Correspondence to: jordan.tubman@mail.mcgill.ca

Simpson et al. [7] carried out impact tests using projectiles produced by mechanically swaging powder, rather than traditional compaction techniques, which both compacts and cold-works the powder. Swaged projectiles exhibit a wider range of properties depending on the degree of swaging and powder size, most notably tending to be more ductile than equivalent compacted samples.

Relatively little work has been done investigating the blast waves produced by supersonic projectile impacts. One of the earliest studies was done by Gee et al. [8]. In this work, a tungsten carbide sphere impacted a rolled homogenous armour target, with no significant contributions from the chemical reaction of the projectile or target. They determined that the blast wave is driven primarily by air entrained by the ejecta. By modeling the blast wave as one produced by a spherical high explosive charge, they estimated that only about 1.4% of the kinetic energy of the impact couples to the blast wave. Further work on the impact of reactive metal projectiles on inert (aluminum oxide) targets was carried out by Idrici et al. [1]. They compared the results using chemically reactive (air, Ar-O_2) and chemically inert (N_2, Ar) environments to isolate the contribution of the chemical energy coupling to the blast wave propagation. The results indicated that less than 0.35% of the potential chemical energy from the combustion of the reactive metal coupled to the blast wave. Despite this low efficiency, the chemical energy release still led to a significant increase in blast wave overpressure for magnesium and aluminum projectiles, as shown in Fig. 1.

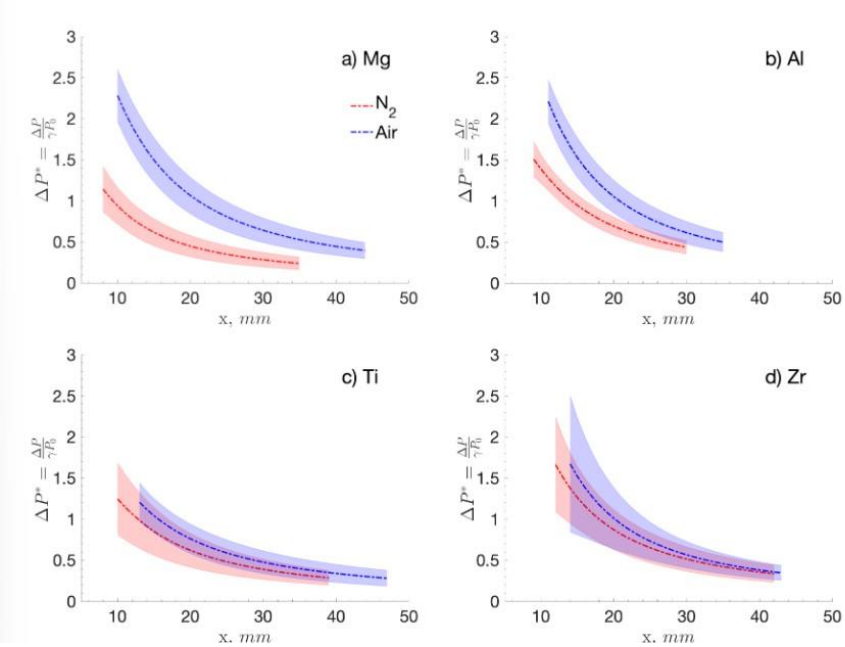

Figure 1: Comparison of the decay in normalized overpressure scaled with γ, $\Delta P*$, as a function of physical distance, x, for blast waves propagating in air (blue) and nitrogen (red) for a) Mg, b) Al, c) Ti, and d) Zr projectiles [1].

The present study extends the earlier work of Idrici et al. [1] by investigating projectiles produced by compacting powders rather than bulk metal projectiles. The powders are compacted to a density less than the theoretical maximum density so that the projectiles have a degree of porosity. It is hypothesized that the porosity can have several effects on the impact process. First, the work done on compacting the pores during impact will heat the air within the pores generating hot spots which may influence the strength of the blast wave formed. Secondly, the particle-particle interfaces within the projectile will influence the subsequent breakup of the projectile. Compacted materials tend to be more brittle than bulk materials, and fragment into smaller sizes on the scale of the powder used. Hence, this work seeks

to determine if the brittle nature and smaller fragments produced with compacted powder projectiles will enhance the reaction rate of the fragmented projectile and more efficiently couple the chemical energy to the blast wave.

The compacted projectiles have a low porosity (<10%), and are prepared from particles ranging in size from 44 – 149 µm. Furthermore, the projectile mass is kept constant across all trials to maintain the velocity and kinetic energy at impact constant. The projectiles impact an inert aluminum oxide target that contributes no chemical energy to the blast. A high-speed Shimadzu HPV-X2 camera is used to record the impact event and visualize the blast wave after impact. The video data is processed in-house to obtain the velocity and Mach number of the blast wave.

2 Numerical simulation of blast wave formation

A preliminary numerical analysis was carried out using the EDEN multiphase hydrocode developed by scientists at Fluid Gravity Engineering Ltd (UK). This code has been extensively validated with experimental results from blast wave experiments with reactive materials (e.g., see Mellor et al. [9]). The computed details of the projectile fragmentation, such as the size of the fragments generated, will, in general, be dependent on the choice of the material and fracture models, and grid resolution. However, hydrocode computations are useful for investigating the general features of the material deformation and blast wave formation on the initial conditions and projectile properties, such as the impact velocity and projectile porosity. A sample calculation is shown in Fig. 2, illustrating the formation of the air blast wave upon impact for a compacted powder projectile. The temperature within the deforming projectile and the strength of the blast wave were found to be a weak function of the initial solid volume fraction of the projectile. Decreasing the initial solid fraction (i.e., increasing the porosity) leads to a small increase in the projectile temperature and blast wave Mach number. The computations provide motivation for comparing the blast wave formation for compacted powder projectiles with that of bulk metal projectiles to validate the predicted dependence on solid volume fraction.

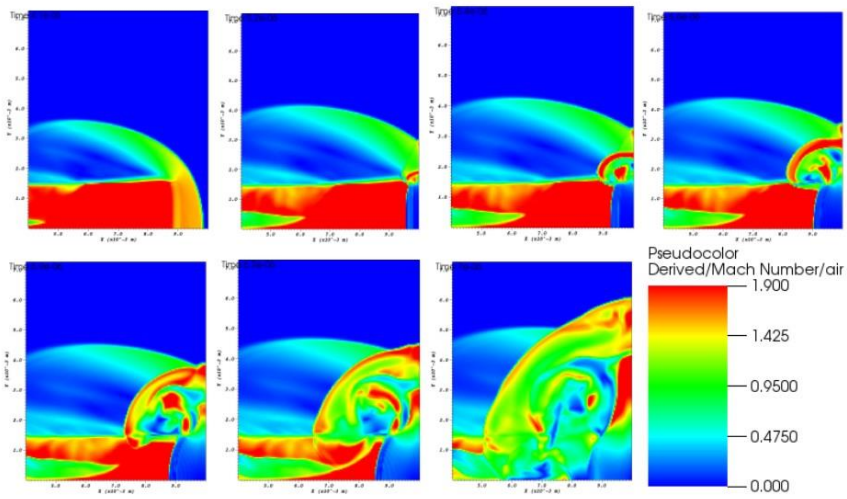

Figure 2: Air Mach number during impact event of compacted aluminum projectile with a rigid wall, from 0.9 µs before impact to 2 µs after impact, calculated with the EDEN hydrocode.

3 Experimental Setup and Diagnostics

Two types of cylindrical projectiles were used in the present work: (1) high-purity (99.5%) bulk aluminum slugs (3.18 mm diameter, 3.18 mm height, ~0.070 g) from Alfa Aesar, and (2) projectiles comprised of compacted aluminum powders with a diameter of 3.1 mm and mass ~0.070 g, where the

height varied depending on the exact mass and compaction level. The projectiles were compacted in-house using a hand-operated press utilizing aluminum powder from Valimet (Stockton, CA, USA) with nominal powder sizes ranging from 44 – 149 µm. The mass and porosity of each projectile were measured, respectively, with a precision scale (±0.1 mg), and pycnometer before each experiment.

The projectiles were attached to a polycarbonate sabot and accelerated with a single-stage helium-driven light-gas gun which is shown schematically in Fig. 3, including the light-gas gun, the test section, the optical diagnostics, and the trigger connections. The impact event and resulting blast wave were visualized with a high-speed Shimadzu HPV-X2 camera recording at 1 Mfps, with an exposure time of 200 ns, with a line-of-sight perpendicular to the target as shown in Fig. 3. Further details regarding the apparatus and test procedure can be found in [1].

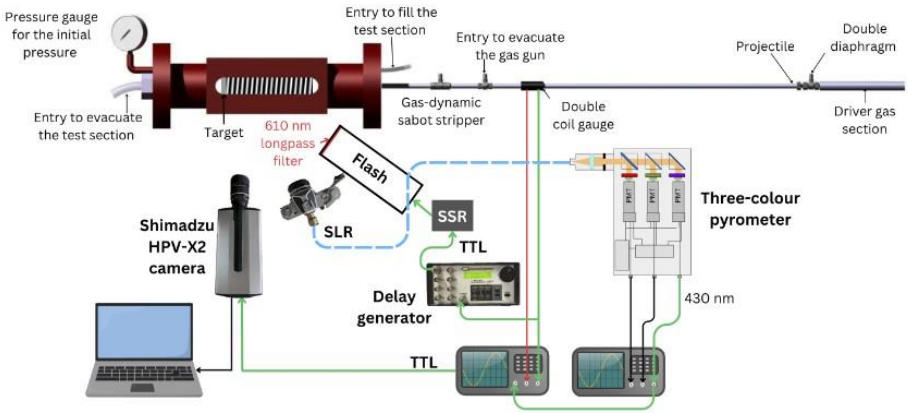

Figure 3: Schematic of the experimental setup including the single-stage light-gas gun, test section, and optical diagnostics. The green lines represent the trigger connections [1].

4 High-Speed Video Processing

The images from the Shimadzu camera are saved as greyscale 16-bit TIFF files. These images are processed by an in-house program that extracts the motion of the blast wave and determines the speed of the shock wave. While not detailed here, the core steps of the image processing procedure, which includes inter-frame image processing, edge tracking, and blast wave fitting, are shown for a typical trial in Fig. 4.

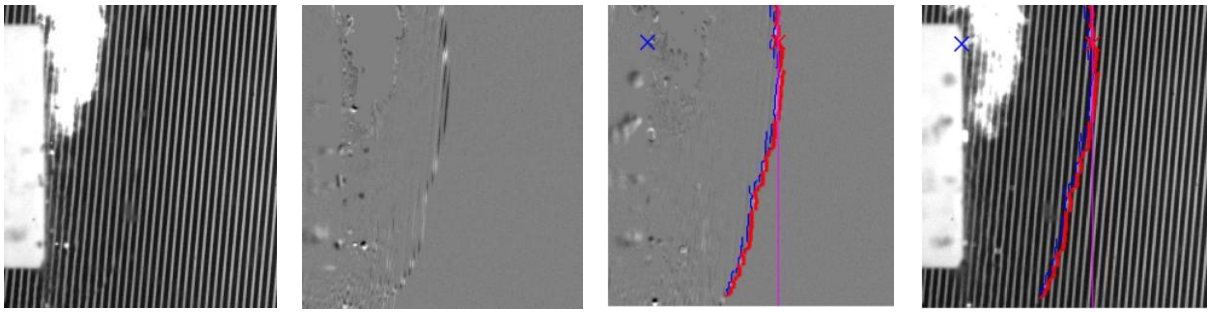

(a) (b) (c) (d)

Figure 4: Image processing of one frame of a typical trial done via in-house program, starting with (a) the raw image, then (b) inter-frame image processing, (c) edge tracking, and (d) overlay of the edge tracking on the raw image.

5. Results and Discussion

The stages of a typical trial are shown in Fig. 5. These stages are the same across all projectile types of interest. The stages in Fig. 5 correspond to, in order left to right: pre-impact, when the projectile is approaching the target; impact with the target; 5 μs after impact; 11 μs after impact, when the blast wave begins to form; and 22 μs after impact, when the blast wave is clearly visible. The video processing begins once the blast wave is first visible.

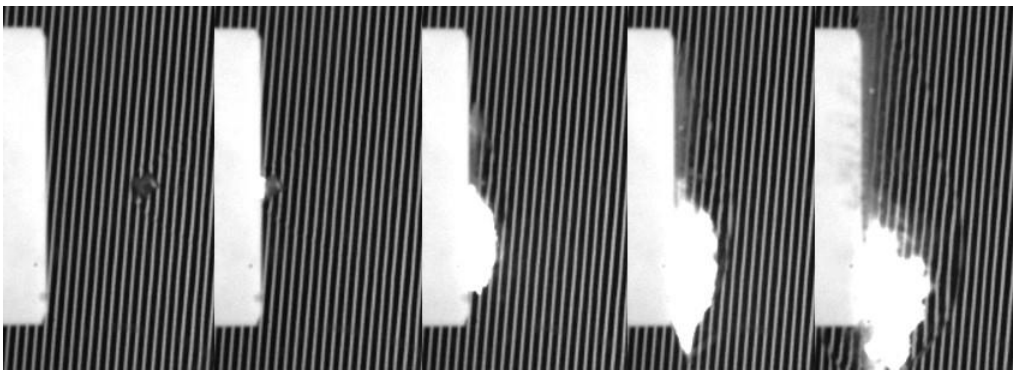

Figure 5: Compacted aluminum (44 μm powder) impact in air at ~1.2 km/s, 1 Mfps and 200 ns exposure (times after impact are -14 μs, 0 μs, 5 μs, 11 μs, and 22 μs, respectively).

Figure 6 shows a comparison of the impact of bulk aluminum and compacted aluminum (H10 powder) projectiles at the same two moments after impact. Images (a) and (c) show the early formation of the blast wave. In the later images (b) and (d), the blast wave has fully developed and moved away from the target, while some fragments remain burning near the target. In the bulk aluminum trial, there are large fragments visible moving up from the target and toward the camera. These large fragments undergo secondary impacts with the walls of the test section, further fragmenting. In the compacted aluminum images, these large fragments are absent. Instead, there is a more prominent cloud of fine fragments located along the face of the target, with no significant secondary impacts. Additionally, a comparison between these two trials seems to indicate that the compacted aluminum powder fragment cloud (Fig. 6d) burns for longer than the bulk aluminum fragments (Fig. 6b), however more trials must be conducted for validation.

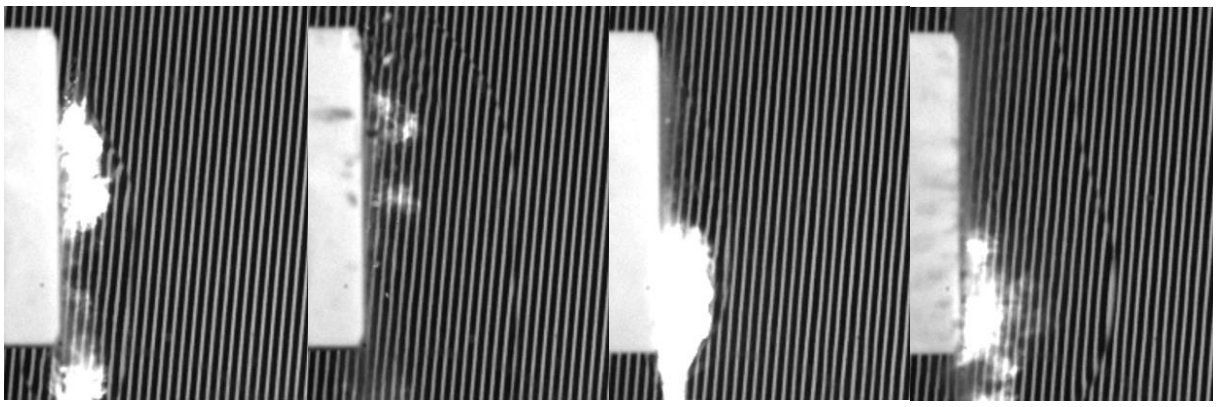

(a) (b) (c) (d)

Figure 6: Comparison of the impact of a bulk aluminum projectile (images a and b) with the impact of projectile comprised of compacted H10 aluminum powder (images c and d). Images (a) and (c) were taken 13 μs after impact, and images (b) and (d) were taken 37μs after impact.

While the video images of these trials suggest some differences in the fragmentation dynamics and combustion of the particles, initial analysis shows no distinct difference between the blast wave trajectories for the bulk and compacted trials, as shown in Fig. 7. Additional trials, including with more powder sizes, are being carried out to validate these results. Results for trials illustrating the dependence of the blast wave strength on the properties of the compacted powder projectiles (in particular, the initial particle size and projectile porosity) will be presented at the meeting.

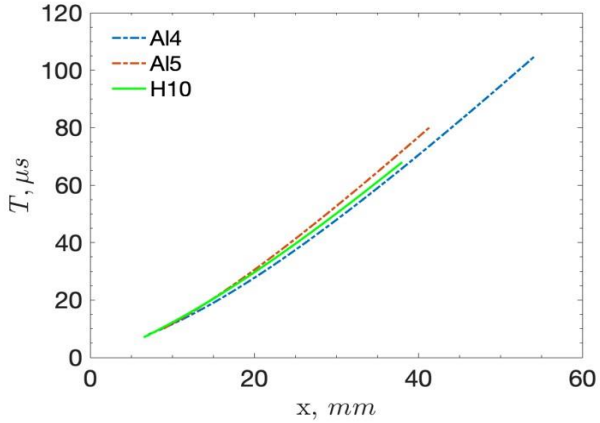

Figure 7: *t-x* diagram of blast wave propagation for preliminary results, where Al4 and Al5 are the trial designations for two trials with bulk aluminum projectiles and H10 corresponds to a trial with compacted H10 aluminum.

References

[1] Idrici D, Goroshin S, Loiseau Frost DL. (2025). Fragmentation and reaction dynamics during ballistic impact of a reactive metal projectile. To appear in Shock Waves Journal, 2025.

[2] Simpson G, Moreno J, Shaeffer M, Ramesh KT. (2023). First contact: Fine structure of the impact flash and ejecta during hypervelocity impact. PNAS Nexus 2: 1-14.

[3] Hooper JP. (2012). Impact fragmentation of aluminum reactive materials. J. App. Phys. 112: 043508.

[4] Tang M, Hooper JP (2018). Impact fragmentation of a brittle metal compact. J. App. Phys. 123: 175901.

[5] Mott NF, Linfoot EH. (2006). A Theory of Fragmentation. Fragmentation of Rings and Shells: The Legacy of NF Mott. Berlin, Heidelberg: Springer Berlin Heidelberg: 207-25.

[6] Kline J, Hooper JP. (2019). The effect of annealing on the impact fragmentation of a pure aluminum reactive material. J. App. Phys. 125: 205901.

[7] Simpson G, Grant J, Weihs TP, Ramesh KT. (2025). Size-dependent fragment shape in high-velocity anvil impact of spherical metal powder-compacts. Acta Materialia 286: 120647.

[8] Gee DJ, Reinecke WG, Levinson SJ. (2007). Blast phenomena associated with high-speed impact. Int. J. Imp. Eng. 34(2): 178–188.

[9] Mellor J, Parry T, Madden E, Burton D, Longbottom A, Cargill S, Lodge T, Tyas A. (2023). Blast analysis of reactive material liners. Proc. 26th International Symposium on Military Aspects of Blast and Shock, Wollongong, Australia.